applied sciences

MDPI

Article

Synergistic Effects of Atomic Oxygen and UV Radiation on Carbon/Carbon Plates at Different Attitude Positions

Andrea Delfini [1,*], Roberto Pastore [1], Marta Albano [2], Fabio Santoni [1], Fabrizio Piergentili [3] and Mario Marchetti [1]

[1] Department of Astronautical, Electrical and Energy Engineering, Sapienza University of Rome, 00185 Rome, Italy; roberto.pastore@uniroma1.it (R.P.); fabio.santoni@uniroma1.it (F.S.); marchettimario365@gmail.com (M.M.)
[2] Italian Space Agency, 00133 Rome, Italy; marta.albano@asi.it
[3] Department of Mechanical and Aerospace Engineering, Sapienza University of Rome, 00185 Rome, Italy; fabrizio.piergentili@uniroma1.it
* Correspondence: andrea.delfini@uniroma1.it

Abstract: Atomic oxygen (AtOx) is a major component of the space environment between 200 and 800 km (LEO—low Earth orbit region) and is the principal source of erosion for exposed aerospace structures. The damage to surface materials is proportional to the AtOx fluence, which depends on altitude, exposure time, orbital inclination, and solar activity, and it is caused by the formation of volatile oxides which do not adhere to the surface; furthermore, the mass loss may also be worsened by UV radiation, which increases the chemical degradation of the exposed material. Carbon/carbon (C/C) is an advanced ceramic composite that is frequently found as a base component of thermal protection systems (TPS), rocket nozzles, or other spacecraft subsystems. In this work, a simulation of the AtOx/UV synergistic effects on C/C plates exposed at different attitude positions were carried out by experimental tests performed at the Aerospace Systems Laboratory (LSA—Sapienza University of Rome) by means of an Atomic Oxygen OS-Prey RF plasma source, which also included a high-power UV-ray generator. The present experimental plan was built on the activity developed during recent years at LSA concerning the study of C/C materials for protecting aerospace structures from thermal shock in re-entry missions. The tests were conceived by considering a fixed time of exposure with a base fluence of 7.6×10^{19} n.s./cm^2, as evaluated from the erosion of the reference samples exposed to AtOx flux at a normal incidence; the simulation of the different attitude positions was then analyzed, also considering the simultaneous effect of UV radiation. The results of the aging ground test suggest the following: (i) C/C oxidation in LEO must be taken into full consideration in the TPS design with reference to protective coating solutions, (ii) the LEO environment simulation is closely related to AtOx/UV combined irradiation, as well as to the spacecraft's in-orbit attitude.

Keywords: LEO space environment; atomic oxygen; UV; synergistic effects; carbon/carbon composite; space systems testing

Citation: Delfini, A.; Pastore, R.; Albano, M.; Santoni, F.; Piergentili, F.; Marchetti, M. Synergistic Effects of Atomic Oxygen and UV Radiation on Carbon/Carbon Plates at Different Attitude Positions. *Appl. Sci.* **2024**, *14*, 5850. https://doi.org/10.3390/app14135850

Academic Editor: Valentino Paolo Berardi

Received: 8 March 2024
Revised: 20 June 2024
Accepted: 2 July 2024
Published: 4 July 2024

1. Introduction

Spacecraft structures undergo considerable exposure to the orbital space environment, which is characterized by conditions of ultra-high vacuum and large thermal variations (entailing problems of outgassing from the exposed surfaces) and by the presence of atomic oxygen (AtOx) and high-energy UV radiation, as well as other phenomena that can cause critical degradation in the performance of materials [1–3]. Atomic oxygen is formed in the low Earth orbital environment (LEO) by photo-dissociation of diatomic oxygen by short-wavelength (<243 nm) solar radiation, which has sufficient energy to break the 5.12 eV O_2 diatomic bond in an environment where the mean free path is sufficiently long (~108 m) so that the probability of reassociation or the formation of ozone (O_3) is small. The issue of AtOx shielding is of crucial interest in the study of the low Earth orbit environment, because this atomic species is highly aggressive toward the organic materials present on the outer

surface of spacecraft, causing physical damage due to erosion and corrosion [4–6]. When a spacecraft travels in LEO (where crewed vehicles and the International Space Station fly), the AtOx formed from the residual atmosphere can react with the exposed surfaces through high-energy impacts (at relative velocities around 8 km/s), which in turn may critically affect the performance of the systems and subsystems. The main AtOx effects on ceramic materials is erosion via chemical reactions and the release of volatile products, resulting in mass loss. Advanced carbon-based composites, such as carbon/carbon (C/C) or carbon/silicon carbide (C/SiC), are the ceramic materials employed in the aerospace industry to deal with the dramatic thermomechanical stress suffered by spacecraft structures during re-entry into the Earth's atmosphere [7–9]. Thanks to their very low thermal expansion, such materials benefit from outstanding chemical stabilities at extreme temperatures and are thus the ideal candidates for reusable integrated space components such as TPS, nozzle throats, and ablation thermal-proof structures [10,11]. In long-term missions, on the other hand, the continuous and extended exposure of spacecraft surfaces to a detrimental oxidative environment must be carefully considered. LEO working conditions, in particular, are responsible for the aging of materials due to the combined effects induced by severe vacuum thermal cycles and harsh UV/AtOx irradiation [12–15]. Such drawbacks may be sufficient to discourage the use of C/C as a re-entry protection material, because significant surface oxidation may lead to so much TPS damage that the main thermomechanical functionality would be compromised. In this work, the preliminary results on the analysis of LEO's environment effects on a commercial C/C material are presented and discussed. The experimental tests were performed by means of a specific facility able to reproduce LEO conditions in terms of AtOx/UV irradiation, analyzing the dependence of C/C erosion damage on both the sample attitude position and the synergic effects of the combined aging agents.

2. Materials and Methods

The AtOx ground-test facility is based on an OS-PREY Plasma Source manufactured by Oxford Scientific Instruments (Abingdon, UK): the system works through the dissociation of molecular oxygen flowing inside a vacuum chamber (allowable pressure ~10^{-3} Pa), controlled by high-precision flowmeters, by means of the energy from a radio frequency source (13.56 MHz). This procedure gives rise to an oxygen-based beam comprised of 99% neutral species (about 60% of monoatomic O and 40% of molecular O_2) with energy in the range of 5–25 eV. A mercury-xenon lamp (Hamamatsu—model LC8 Lightning Cure (Hamamatsu Photonics, Shizuoka, Japan)) was adopted to simulate UV irradiation: this device was mounted on the AtOx chamber, providing high-intensity UV line spectra with an elliptical reflector (UV cold mirror (Abrisa Technologies, Santa Paula, CA, USA)) with reflectivity higher than 90% in the UV range and a quartz light guide with UV transmittance. The spectral emittance field was in the 200–600 nm range, with a maximum emission value of 365 nm, and the radiation intensity of the lamp system was 410 mW/cm^2 (around 10 Suns) at a distance of 30 mm with an aperture size of 20 mm. The experimental facilities and setup conditions are shown in Figure 1. During the tests, the mean environmental temperature was recorded by means of a sensor placed on the sample holder, as reported in the plot of Figure 2. The temperature rise was a consequence of the combined use of AtOx and UV rays. The environment reached 100 °C in around two hours with a non-linear gradient that was very steep during the first hour; in the remaining exposure time (test duration ~11 h), the temperature asymptotically approached the maximum value of about 105 °C.

The C/C material samples tested were obtained from a Mitsubishi carbon/carbon slab obtained through the waterjet cutting method, providing several pieces measuring 3 × 6 cm and about 4 mm in thickness. The tests were performed considering a fixed time of exposure, with a AtOx base fluence of 7.6 × 10^{19} n.at./cm^2 as measured by the normal irradiation of the reference samples (Kapton HN, [16]). The simulation of the different attitudes was made possible by the axial rotation of the sample holder at four tilted positions (15°, 30°, 45°, and 60°) with respect to the AtOx beam direction. The

analysis of the surface damage was carried out by measuring the mass loss and consequent evaluation of the erosion yield parameter. The basic background lies within the operative expression of the erosion rate E_Y, which is given in [cm^3/n.at.]—i.e., as the eroded volume for an impinging atom—by the relationship:

$$E_Y = \frac{\Delta M}{\rho \cdot F \cdot A} \quad , \qquad F = f \cdot \Delta t \tag{1}$$

where ΔM is the mass loss [g], ρ is the material density [g/cm^3], A is the exposed surface [cm^2], and F is the fluence, which is given as the total number of impacts per surface unit [n.at./cm^2]; the latter quantity takes into account the whole time of exposure Δt [s] and is typically related to a supposed constant AtOx flux f, which is expressed in [n.at./(s·cm^2)], as indicated by the second expression in Equation (1). On this basis, a physical modeling was introduced in order to study how the mechanism (and in turn, the measurement) of AtOx erosion may be dependent on the orientation of the exposed surface with respect to the direction of the AtOx flux (i.e., the direction of the spacecraft motion) as well as on the concomitant vacuum UV radiation.

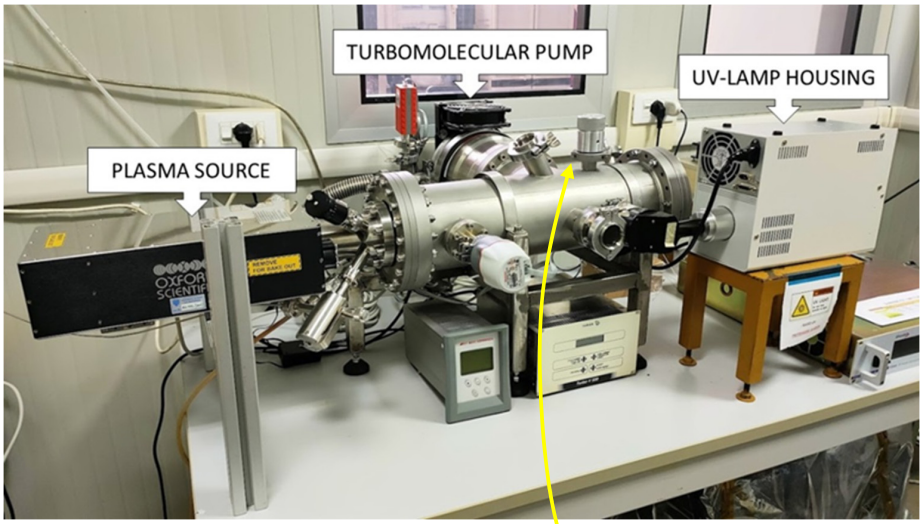

(**a**)

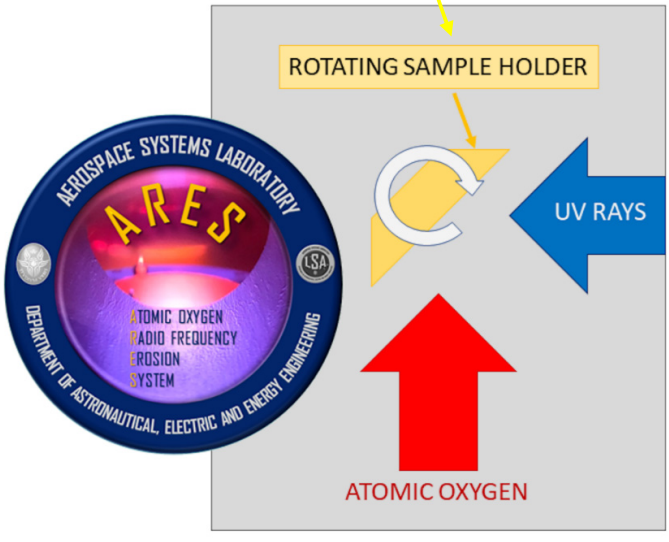

(**b**)

Figure 1. AtOx/UV experimental facilities at the Aerospace Systems Laboratory (LSA—Sapienza University of Rome) (**a**) and setup conditions showing the control of sample attitude variation (**b**).

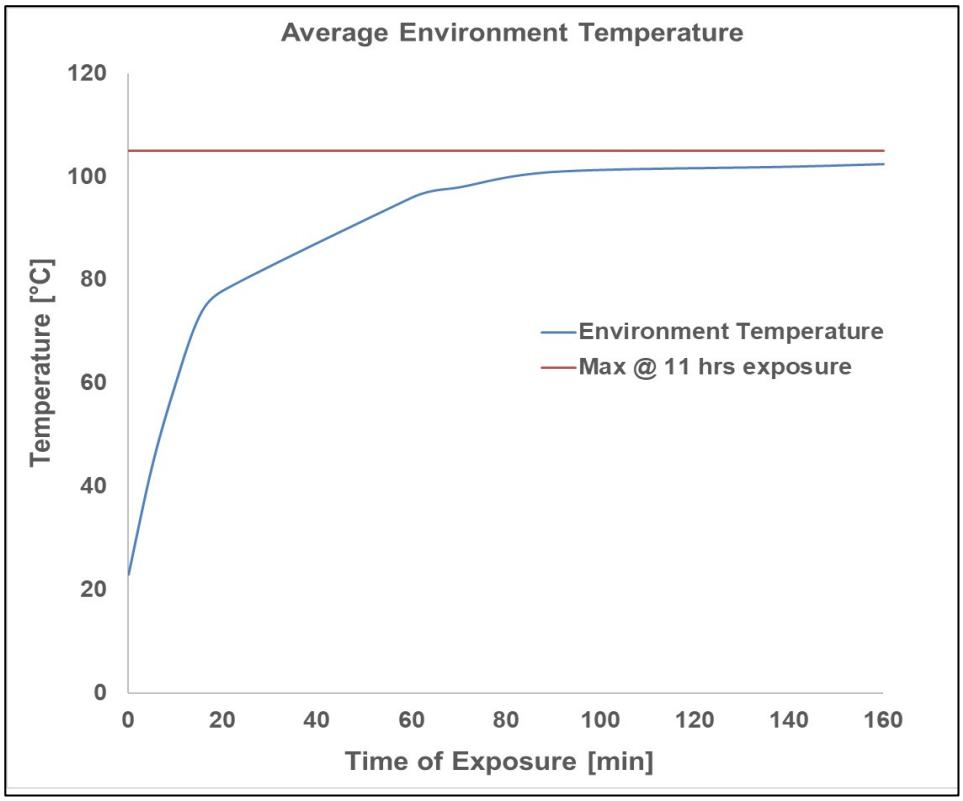

Figure 2. AtOx/UV test: mean detected environmental temperature.

3. Results and Discussion

In Table 1, we report the preliminary experimental results obtained by testing the reaction of the C/C samples to the synergic irradiation of AtOx and UV at five progressive attitudes (Figure 3). Three specimens were exposed to the AtOx/UV combined flux for each attitude position for a total of 15 ground tests in the experimental campaign The samples' mass was measured by means of a high-precision Mettler–Toledo micro-balance of sensitivity 10^{-6} g, as suggested by the practice standard [16]; mass loss values are given to a 10^{-5} g precision as the result of statistical uncertainty by two measurements (sample weight before and after the test), three samples for each position, and three recording operations for each sample. The time of exposure was 39,600 s (11 h) for an AtOx flux of about 1.9×10^{15} n.s./(s·cm^2), as estimated by the analyzed fluence effects on the polymide (Kapton HN) reference samples. The measured density of the C/C samples varied around 1.35 g/cm^3, whereas the area exposed to irradiation might be different each time due to unavoidable fluctuations related to the clamping system adopted (Figure 4, images on the left), varying in the 11–17 cm^2 range.

Table 1. AtOx/UV irradiation test over the C/C samples at different attitudes; the values reported represent the average of three measurements for each position.

Attitude Test	Mass Loss (g)	Erosion Yield (cm^3/n.at.)
0°	0.01215	9.694×10^{-24}
15°	0.01188	9.650×10^{-24}
30°	0.01064	9.535×10^{-24}
45°	0.00924	7.162×10^{-24}
60°	0.00540	3.047×10^{-24}

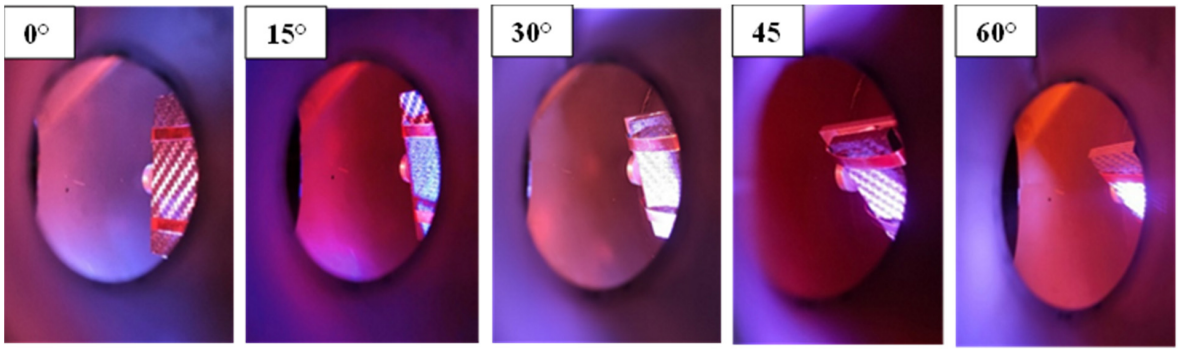

Figure 3. C/C samples under AtOx/UV irradiation at different angles of attack with respect to the AtOx beam (the pictures were taken from the window just below the handle system for the holder rotation; see Figure 1).

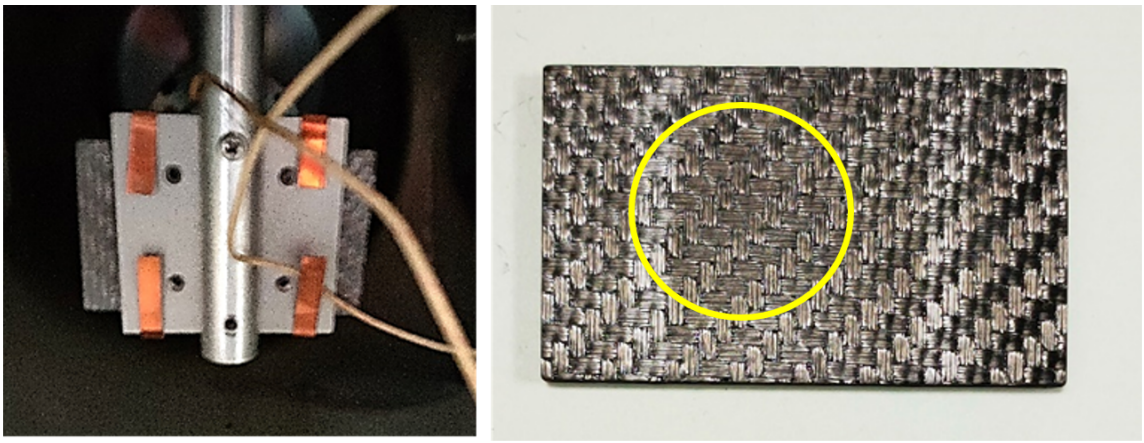

(**a**)

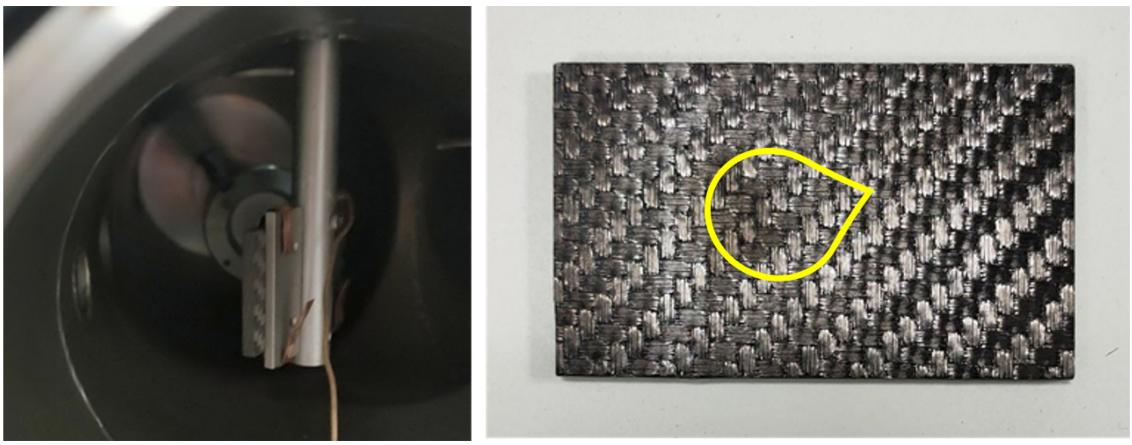

(**b**)

Figure 4. C/C sample clamping before the test (**left**) and picture after the test (**right**) for 0° (**a**) and 60° (**b**) attitudes; the area visibly affected by the AtOx irradiation is highlighted.

The changing attitude clearly resulted in higher erosion at a lower angle of attack from AtOx—i.e., in conditions closer to the normal incidence. Nevertheless, starting from the result obtained in the tests performed at the 0° attitude condition, the observed drop of AtOx erosion yield was not merely consistent with a typical tilt-angle behavior law, thus suggesting that a more particular effect of AtOx impact orientation on erosion should be envisaged. The erosion may also be increased by simultaneous UV irradiation. A modeling

schematization was introduced in order to attain the following: (i) overall, to approach the issue of the AtOx erosion phenomena in generic conditions, and (ii) specifically, to give a physical interpretation of the experimental results obtained.

The simplified relationships reported in Equation (1) can be directly arranged to retrieve a differential expression for the mass eroded as a function of time:

$$\delta M(t) = \rho \cdot A \cdot E_Y \cdot f(t) \cdot \delta t \tag{2}$$

where the generalized flux vs time relation $f\ (t)$ shall be evaluated for the computation of the total mass eroded by the AtOx impacts between two instants of time (for example, the start and the end of a mission) t_A and t_B, as:

$$\Delta M(t_A \rightarrow t_B) = \rho \cdot A \cdot E_Y \int_{t_A}^{t_B} f(t) dt \tag{3}$$

In this framework, the erosion rate is correctly viewed as an intrinsic property of the material, while the surface inclination with respect to the AtOx fluence direction (i.e., the spacecraft motion) is directly included within the generalized function $f(t)$. In other words, in addition to the AtOx fluence amount that depends on predefined conditions (such as orbit altitude and solar activity), the expected erosion relies on the effective fluence impinging on the surface considered: this continues to shrink at higher attitudes (see right images in Figure 4); in other words, the radiation intensity must be considered to decrease at higher-tilting angles. Thus, referring to Figure 5, the effective flux in Equation (3) may be expressed in a straightforward way as:

$$f(t) = f_0[\hat{\boldsymbol{v}} * \hat{\boldsymbol{n}}]_t = f_0 \cos[\alpha(t)] \tag{4}$$

where f_0 represents the given (maximum) value of the AtOx flux (at fixed external conditions, as mentioned above), whereas the inner product between normal to the exposed surface and the velocity unit vector (spacecraft movement) requires knowing precisely the attitude variation along the time span considered (obviously, Equation (4) holds for $-\pi/2 < \alpha < \pi/2$, because the AtOx flux would be ineffective elsewhere—i.e., when the surface is ideally 'shaded' by the vehicle motion itself). The combination of Equations (4) and (5) and the modeling extension shifts readily to express, for instance, the amount of mass eroded during a mission consisting of several steps '*i*' at predefined altitudes and known solar activities ($f_{0,i}$), as well as scheduled orbit inclinations (α_i), written as:

$$\Delta M = \sum_i \Delta M_i = \rho \cdot A \cdot E_Y \sum_i f_{0,i} \cdot \cos \alpha_i \cdot \Delta t_i \tag{5}$$

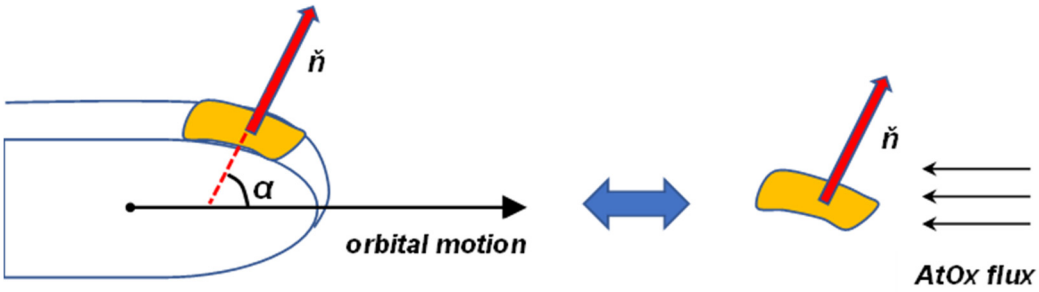

Figure 5. Mutual orientation schematics between the spacecraft outer surface and the AtOx flux.

Returning to the AtOx erosion measurements, with these assumptions a first attempt to retrieve the rate vs attitude values reported in Table 1, the value is given by the trivial expression:

$$E_Y(\alpha) = E_Y(0^\circ) \cdot \cos \alpha \tag{6}$$

where the material 'zero' erosion rate is calculated from the pre-assessed value of the AtOx fluence specific to the adopted setup: because the latter is obtained by the frontal irradiation of reference specimens, Equation (6) is actually complementary to Equation (4), following the conventional physical concept of 'field flow' across a surface (f_0 representing the scalar intensity, that is, the flux at the frontal incidence and α being the tilt angle between normal to surface and local field direction).

From the plots reported in Figure 6, it is clear that a simple (half) sinusoidal law (red-dotted curve) only partially fits the experimental results (black dots sequence), which is significant for both under- and over-estimating discrepancies. In particular, the sharp decrease in erosion at higher attitudes suggests that more effects of the AtOx damping arise by surface tilting than the simple one just considered. That is, the reduction in the effective flux occurred not only because the AtOx radiation intensity—in terms of 'number of impacting particles per unit of time/surface'—actually continued to decrease when moving off the normal incidence, but also because the erosion capability itself was fairly restrained, given that (for the same energy) the AtOx impact momentum was transferred less effectively to the exposed surface due to a non-negligible tangential component.

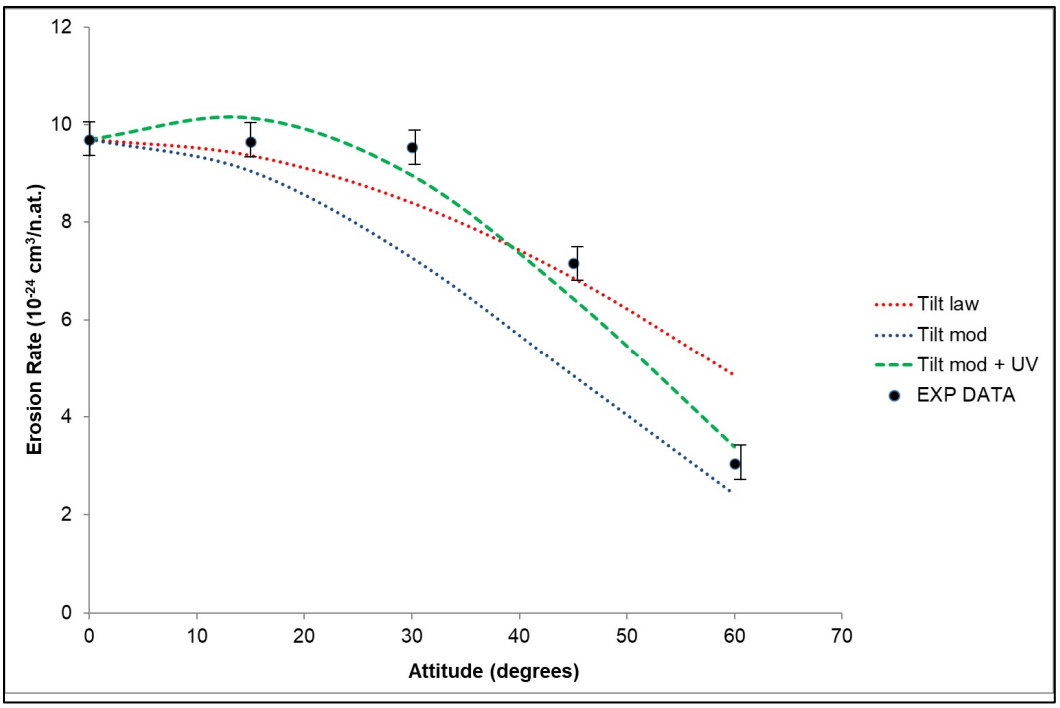

Figure 6. AtOx/UV erosion of the C/C samples at different attitudes: experimental measurements and physical modeling.

We will not here go into the complex details of the chemical reactions involved in the erosion mechanism because they are intuitively comprehensible, given that the penetration depth of a colliding oxygen atom is statistically higher for a direct bump, while tending to be lower for a slitter interaction. This same trend holds for the probability of matter extraction from the surface, passing from inelastic impact dynamics to scattering behavior. Without loss of the properties, such a double effect may be tackled at first by iterating the attitude damping factor, thus accounting for a faster decrease in the erosion yield ($E_Y \propto \cos^2\alpha$): the corresponding modified tilt law (blue-dotted curve in Figure 6) describes well the low erosion at an attitude above 45° but clearly underestimates the AtOx flux effectiveness at intermediate surface orientations. A further parametric correction must then be introduced in order to take into account how the UV irradiation would increase the main AtOx erosion mechanism. Such a synergic effect has been widely observed [12,17–19]; nevertheless, due to both the high complexity of the phenomena and the lack of a full,

reliable database, a systematic analysis of an AtOx-damaging enhancement by concomitant effects (such as surface chemical etching induced by vacuum UV and thermal dilatation) is still under investigation [20]. Preliminarily, by similar considerations made for the AtOx fluence's effectiveness, the UV boosting factor is expected to be dependent on the mutual orientation between the radiating stream and the surface of the material: it is easy to see that, within the adopted test setup (see Figure 1), the AtOx and UV beams are approximately shifted by $\pi/2$ from each other; thus, the relationship between erosion rate and attitude becomes:

$$E_Y(\alpha) = E_Y(0^\circ) \cdot \cos^2 \alpha \cdot (1 + k_{uv} \sin \alpha) \tag{7}$$

where the single, dimensionless parameter introduced to estimate the AtOx/UV coupling can be optimized in order to fit the experimental data. A value of $k_{uv} \sim 0.5$ is retrieved by a standard regression method to minimize the whole discrepancy with the measurements, as shown in Figure 6 (green dashed curve): interestingly, the proposed modeling successfully explains how a relatively low UV exposure could amplify the damage caused by frontal impinging AtOx, whereas a more direct UV irradiation would be almost irrelevant (at least in terms of the material's mass loss) if the AtOx erosion capability is itself suppressed by high-tilted attitude conditions.

By recalling Equations (3)–(5), a generalized expression aimed at predicting the full amount of mass eroded during a defined time/orbit exposure to the AtOx/UV environment is then given as:

$$\Delta M = \sum_i \Delta M_i = \rho \cdot A \cdot E_Y(0^\circ) \cdot \sum_i \left\{ \int_{t_{i-on}}^{t_{i-off}} \left[f_{0,i} \cdot ([\hat{\boldsymbol{v}} * \hat{\boldsymbol{n}}]_t)^2 \cdot (1 + k_{uv,\,i} \cdot [\hat{\boldsymbol{r}}_{uv} * \hat{\boldsymbol{n}}]_t) \right] \cdot dt_i \right\} \tag{8}$$

which, beyond the constitutive structure's parameters (density, exposed area, and nominal AtOx erosion rate), requires knowing the AtOx flux and the UV-enhancing factor for each time step i, as well as the time-variation attitude with respect to both the orbital motion and the UV source ($\hat{\boldsymbol{r}}_{uv}$) along each mission phase.

The analysis presented here should be of aid for gaining clues to the well-known discrepancies between AtOx in-flight experiments and ground simulation results, which are frequently up to one order of magnitude or more and in both directions [13,17–22]. For example, in [13], a value of an AtOx reactivity coefficient of 0.63×10^{-24} cm^3/n.at. is reported as delivered in the spacecraft flown for STS-8 for basal-oriented graphite material, while a much greater result of 9.2×10^{-24} cm^3/n.at. is given by the ground simulation experiment; in contrast, the same benchmark review reports values in the range of 2.0–4.7 $\times 10^{-25}$ cm^3/n.at. as found in the LDEF spacecraft flown for FEP Teflon specimens, while a reduced coefficient of 0.7–0.8 $\times 10^{-25}$ cm^3/n.at. is reported by the ground simulation experiment. Damaging underestimations are likely to be due to real conditions of low attitude and direct UV exposure (for example, within the setup of AtOx fluence and UV ray intensity adopted, the potential AtOx erosion may effectively be up to 50% greater); on the contrary, an overstated aging will be wrongly expected if the ground-simulated erosion rates (commonly evaluated by means of normal AtOx irradiation tests) are applied to long-term, in-flight stages with high attitude conditions. This can be of key importance for spacecraft C/C-based TPS design, because the crucial functionality of these components in re-entry missions requires an accurate safety limit assessment. For instance, supposing that the tested C/C material is analyzed to be employed as the exposed layer of re-entry systems, a reliable failure alert may be set off when the component is damaged by LEO agents at 30% of its thickness: a simple evaluation of erosion depth rate (μm/s) is made possible by the experimental results reported, stating that a mechanical breakdown is expected to occur after less than two months within the operative conditions of aligned AtOx/UV irradiance, while the same structure is believed to withstand LEO agents for more than one year by addressing particular spacecraft design and mission dimensioning.

In any case, the most recent findings establish that commercial C/C materials cannot be considered as fully suitable for long-term LEO re-entry missions without specific surface antioxidative reinforcement: it has been confirmed that advanced coating treatments are necessary in order to provide modified C/C bulk materials with improved AtOx resistance (e.g., $E_Y < 10^{-24/-25}$ cm^3/n.at.), as has been previously reported elsewhere [14,23].

4. Conclusions

In this study, the characterization of an advanced ceramic material, such as a C/C composite in terms of erosion by AtOx high-energy impact, was presented, focusing on both the effect of the material's surface/incident flux mutual orientation (attitude) and the influence of synergic UV irradiation on the erosion mechanism. LEO space system deterioration and failure due to AtOx-induced processes are today not yet fully known, due to the many mechanical and chemical parameters involved in such complex dynamics. The present research represents a novel attempt to clarify the critical roles of spacecraft attitude and synergic AtOx/UV irradiation, with the aim of providing a technical baseline to explain the significant gap noticed so far between in-flight experiments and ground-test simulations. The measurements here reported demonstrate evidence that, during a whole LEO mission, favorable attitude positions (in relation to the mutual orientation between the sensitive surface and the ram direction—i.e., AtOx flux) may successfully inhibit the detrimental AtOx oxidative effects on C/C structures, while, on the other hand, a critical boosting of the AtOx erosion may arise as a consequence of even weak exposure to highly energetic UV rays. Semi-empirical modeling was thus introduced in order to give a physical interpretation of the experimental results obtained within the adopted LEO simulation setup; both functional and quantitative considerations attest to the reliability of the theoretical approach proposed, thus establishing the coupling between the materials' constitutive space properties (measured by ground testing) and the specific mission parameters as an effective strategy for predicting the actual behavior of aerospace structures in the LEO environment. Tackling this task is expected to be extremely useful for improving the design of spacecraft's protective systems, with particular regard to C/C-based advanced TPS for re-entry vehicles and, more generally, for applications in large space structures operating during long-term missions within LEO regions, such as the ISS.

Author Contributions: Conceptualization, A.D. and R.P.; Methodology, R.P.; Validation, M.A.; Investigation, A.D. and R.P.; Writing—original draft, A.D. and R.P.; Supervision, F.S., F.P. and M.M. All authors have read and agreed to the published version of the manuscript.

Funding: This research received no external funding.

Institutional Review Board Statement: Not applicable.

Informed Consent Statement: Not applicable.

Data Availability Statement: The data are contained within the article.

Conflicts of Interest: The authors declare no conflicts of interest.

References

1. Finckenor, M.M.; de Groh, K.K. *Space Environmental Effects—A Researcher's Guide to: International Space Station*; NASA ISS Program Science Office: Houston, TX, USA, 2015.
2. Yang, J.C.; de Groh, K.K. Materials Issues in the Space Environment. *MRS Bull.* **2010**, *45*, 12–19.
3. Dever, J.A.; Banks, B.A.; de Groh, K.K.; Miller, S.K. Degradation of Spacecraft Materials. In *Handbook of Environmental Degradation of Materials*; Kutz, M., Ed.; William Andrew Publishing: Norwich, NY, USA, 2005; pp. 465–501. [CrossRef]
4. Tagawa, M.; Yokota, K. Atomic oxygen-induced polymer degradation phenomena in simulated LEO space environments: How do polymers react in a complicated space environment? *Acta Astronaut.* **2008**, *62*, 203–211. [CrossRef]
5. Hooshangi, Z.; Feghhi, S.A.H.; Saeedzade, R. The effects of low earth orbit atomic oxygen on the properties of Polytetrafluoroethylene. *Acta Astronaut.* **2016**, *119*, 233–240. [CrossRef]
6. Peters, P.N.; Linton, R.C.; Miller, E.R. Results Of Apparent Atomic Oxygen Reactions On Ag, C, And Os Exposed During the Shuttle STS-4 Orbits. *Geophys. Res. Lett.* **1983**, *10*, 569–571. [CrossRef]

7. Lyle, K.H.; Fasanella, E.L. Permanent Set of the Space Shuttle Thermal Protection System Reinforced Carbon-Carbon Material. *Compos. Part A Appl. Sci. Manuf.* **2009**, *40*, 702–708. [CrossRef]
8. Balakrishnan, D.; Kurian, J. Material Thermal Degradation Under Reentry Aerodynamic Heating. *J. Spacecr. Rocket.* **2014**, *51*, 1319–1328. [CrossRef]
9. Christiansen, E.L.; Friesen, L. Penetration Equations for Thermal Protection Materials. *Int. J. Impact Eng.* **1997**, *20*, 153–164. [CrossRef]
10. Krenkel, W.; Brendt, F. C/C-SiC Composites for Space Applications and Advanced Friction Systems. *Mater. Sci. Eng. A* **2005**, *412*, 177–181. [CrossRef]
11. Albano, M.; Delfini, A.; Pastore, R.; Micheli, D.; Marchetti, M. A New Technology for Production of High Thickness Carbon/Carbon Composites for Launchers Application. *Acta Astronaut.* **2016**, *128*, 277–285. [CrossRef]
12. Grossman, E.; Gouzman, I. Space Environment Effects on Polymers in Low Earth Orbit. *Nucl. Instrum. Methods Phys. Res. B Beam Interact. Mater. At.* **2003**, *208*, 48–57. [CrossRef]
13. Reddy, M.R. Review—Effect of Low Earth Orbit Atomic Oxygen on Spacecraft Materials. *J. Mater. Sci.* **1995**, *30*, 281–307. [CrossRef]
14. Delfini, A.; Santoni, F.; Bisegna, F.; Piergentili, F.; Pastore, R.; Vricella, A.; Albano, M.; Familiari, G.; Battaglione, E.; Matassa, R.; et al. Evaluation of atomic oxygen effects on nano-coated carbon-carbon structures for re-entry applications. *Acta Astronaut.* **2019**, *161*, 276–282. [CrossRef]
15. Klein III, T.F.; Lesieutre, G.A. Space Environment Effects on Damping of Polymer Matrix Carbon Fiber Composites. *J. Spacecr. Rocket.* **2000**, *37*, 519–525. [CrossRef]
16. Standard Practices for Ground Laboratory Atomic Oxygen Interaction Evaluation of Materials for Space Applications. Available online: https://www.astm.org/e2089-15r20.html (accessed on 16 August 2017).
17. Zhao, X.H.; Shen, Z.G.; Xing, Y.S.; Ma, S.L. An experimental study of low earth orbit atomic oxygen and ultraviolet radiation effects on a spacecraft material—Polytetrafluoroethylene. *Polym. Degrad. Stab.* **2005**, *88*, 275–285. [CrossRef]
18. Banks, B.A.; Rutledge, S.K.; Paulsen, P.E.; Steuber, T.J. *Simulation of the Low Earth Orbital Atomic Oxygen Interaction with Materials by Means of an Oxygen Ion Beam*; NASA TM-101971; NASA: Washington, DC, USA, 1989.
19. Grossman, E.; Gouzman, I.; Lempert, G.; Noter, Y.; Lifshitz, Y. Kapton as a Standard for Atomic Oxygen Flux Measurement in LEO Ground Simulation Facilities: How Good Is It? In *Protection of Materials and Structures from Space Environment. Space Technology Proceedings*; Kleiman, J.I., Iskanderova, Z., Eds.; Springer: Dordrecht, The Netherlands, 2004; Volume 5, pp. 379–390. [CrossRef]
20. Banks, B.A.; Steuber, T.J.; Norris, M.J. *Monte Carlo Computational Modeling of the Energy Dependence of Atomic Oxygen Undercutting of Protected Polymers*; NASA TM-207423; NASA: Washington, DC, USA, 1998.
21. Banks, B.A.; de Groh, K.K.; Rutledge, S.K.; DiFilippo, F.J. *Prediction of In-Space Durability of Protected Polymers Based on Ground Laboratory Thermal Energy Atomic Oxygen*; NASA TM-107209; NASA: Washington, DC, USA, 1996.
22. Banks, B.A.; de Groh, K.K.; Miller, S.K. *Low Earth Orbital Atomic Oxygen Interactions with Spacecraft Materials*; NASA TM-213400; NASA: Washington, DC, USA, 2004.
23. Delfini, A.; Pastore, R.; Santoni, F.; Piergentili, F.; Albano, M.; Alifanov, O.; Budnik, S.; Morzhukhina, A.V.; Nenarokomov, A.V.; Titov, D.M.; et al. Thermal analysis of advanced plate structures based on ceramic coating on carbon/carbon substrates for aerospace Re-Entry Re-Useable systems. *Acta Astronaut.* **2021**, *183*, 153–161. [CrossRef]